



Cite this: *RSC Adv.*, 2021, **11**, 17399

Novel micron-thick brick cladding of polyfluorosilicone acrylates, a case study of conservation of historic brick wall in Hongcun village[†]

Jian Hao, ^{*ab} Liyan Yu,^a Yongmei Cui,^{*ab} Wen Wan^a and Junyi Huang^{*c}

A micron-thick (3–5 μm) and transparent cladding technique based on the environment friendly dimethyl carbonate solution of newly developed polyfluorosilicone acrylates was successfully applied to restore the surface of brick walls of a historic house which has been severely eroded by damp and mildew for more than 300 years in Hongcun village, one of the World Heritage sites in China. The restoration followed the rule of repairing old as old before. The cladding made from the copolymerized polyfluorosilicone acrylate resin, which mainly contained the chain fragments of dodecafluoroheptyl methacrylate and 3-(trimethoxysilyl) propyl methacrylate, permeated through the surface of old brick with an average depth of 14.5 mm in this case study, and provided an ultrathin and efficient covering of the microstructure of the shallow surface layer of old bricks and resulted excellent water-proof, moisture-proof, mildew-proof and long-lasting weather resistance effects. The water contact angle of the treated surface of the old bricks reached 133°, the water absorption of treated bricks was reduced from 16.1 wt% to 2.8 wt% after soaking in water for 24 h.

Received 11th December 2020
 Accepted 29th April 2021

DOI: 10.1039/d0ra10434e

rsc.li/rsc-advances

1. Introduction

The typical problems encountered by buildings near a water source are damp and mildew on the walls. Located at the foot of Huangshan Mountain in China, the Hongcun ancient building complex, which was inscribed in the World Heritage List, was built in the first year of Shaoxing in the Southern Song Dynasty (AD 1131) and most of the buildings were built near the water source. After hundreds of years of baptism, most of the walls of these buildings are seriously damaged by damp and mildew. The most of buildings in Hongcun have brick-wood structures. The situation of the corrosion of brick walls caused by moisture and mildew has been more and more serious and threatened the safety of the building structures (Fig. 1). Thus, the development of a target protective material and technology for the conservation of the external walls of the historic house which meanwhile meets the principles of cultural relics conservation of repairing old as old before is the key to the conservation of such cultural relics.¹

^aDepartment of Chemistry, Shanghai University, Shanghai, 200444, P. R. China.
 E-mail: jhao@shu.edu.cn; ymcui@shu.edu.cn

^bInstitute for the Conservation of Cultural Heritage, Shanghai University, Shanghai, 200444, P. R. China

^cSchool of Life Sciences, Shanghai University, Shanghai, 200444, P. R. China. E-mail: jy-huang@shu.edu.cn

† Electronic supplementary information (ESI) available. See DOI: [10.1039/d0ra10434e](https://doi.org/10.1039/d0ra10434e)

Alkoxysilanes are the most widely used protective materials for the conservation of such historic houses during the past decades.^{2–5} However, tendency to crack during shrinkage and drying due to their brittleness,⁶ long curing time⁷ and slight colour alteration are often observed when alkoxysilanes are used. By contrast, the reported fluorosilicone polymers^{8,9} have some advantages in terms of better mechanical strength, weather resistance, and shorter curing time, but their hydrophobicity is poor, which limit their application in the conservation of masonry.

In this work, a series of novel polyfluorosilicone acrylates with good comprehensive properties were synthesized by radical initiated solution polymerization of dodecafluoroheptyl methacrylate, 3-(trimethoxysilyl)propyl methacrylate and



Fig. 1 (a) Hongcun village of Anhui province; (b) the brick samples were from a historic house in Hongcun village, Anhui province, there was no difference between the four bricks, the water content of four bricks was 13 wt%.

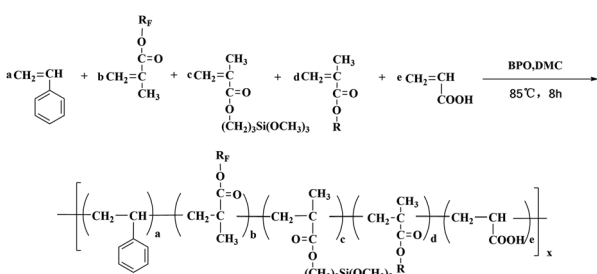


normal acrylates for the conservation of the surface of brick wall of historic houses. The styrene was selected for its high pencil hardness and low-cost. The isobornyl methacrylate was added to lower the viscosity of the polymer solution and increase the pencil hardness of the coating. The 3-(trimethoxysilyl)propyl methacrylate was introduced for improving the water resistance, adhesion, hardness, thermal stability, chemical resistance, weather resistance and water vapor permeability of the coatings. The presence of fluorinated moiety, Si-O-Si cross-linking network and hydroxyl groups ensured the polymer film with outstanding water repellency, water resistance, thermal stability, chemical resistance, antibacterial and fungistatic properties, weather resistance and adhesive performance. Compared to other fluorosilicone polymers, the polyfluorosilicone acrylates prepared in this work presented excellent adhesive performance, water repellency, water resistance and weather resistance. The preliminary results in Hongcun village showed that the cladding technique is an efficient approach for the improved protection of the brick wall of the historic house from water, damp and mildew.

2. Experimental

2.1. Materials

Trifluoroethyl methacrylate (G03, 96+%), hexafluorobutyl methacrylate (G02, 96+%) and dodecafluoroheptyl methacrylate (G04, 96+%), were supplied by XEOGIA Fluorine-Silicon Chemical Co., Ltd. Isobornyl methacrylate (IBOMA, 85%) was purchased from Sahn Chemical Technology Co., Ltd. Styrene (St, 99.5+%), acrylic acid (AA, 99.5+%) and benzoyl peroxide (BPO, 99.7+%) were from Sinopharm Chemical Reagent Co., Ltd. 3-(Trimethoxysilyl)propyl methacrylate (KH-570, 98%) was provided by Jining Huakai Resin Co., Ltd. Dimethyl carbonate (DMC, 99+%) and ethanol (EtOH, 99.5+%) were supplied by Shanghai Gaoyun Chemical Co., Ltd. All reagents and solvent were used as received without further purification. The old bricks with dimensions 22 cm × 10 cm × 4 cm were obtained from Hongcun village, Yixian county, Anhui province, 300 years ago and cut into 5 cm × 5 cm × 1 cm for water vapor permeability test, 1 cm × 1 cm × 2 cm for the water contact angle measurement, water absorption by total immersion, freeze-thaw cycles test and soluble salts aging test.



Scheme 1 Polymerization of polyfluorosilicone acrylates. $R_F = CH_2-CF(CF_3)CHCF(CF_3)_2$, CH_2CF_3 , $CH_2CF_2CHFCF_3$; $R = C_{10}H_{17}$, x is a positive integer.

Table 1 The recipes of the polyfluorosilicone acrylates

Monomers	Content (wt%) ^a			
	FS/S-5	FS/S5	FS/S-10	FS/S-15
G04	30	30	30	30
St	55	65	50	45
IBOMA	10	0	10	10
KH-570	5	5	10	15
AA	3	3	3	3
BPO	0.8	0.8	0.8	0.8

^a Accounted for the percentage of total.

2.2. Synthesis of polyfluorosilicone acrylates

The polyfluorosilicone acrylates were prepared *via* a radical initiated solution polymerization. All the polymerizations were carried out in a 250 mL three-neck flask equipped with a reflux condenser, a mechanical stirrer, an inlet for nitrogen gas and a thermometer in the oil bath. The polyfluorosilicone acrylates were synthesized as shown in Scheme 1. The recipes of the polyfluorosilicone acrylates were listed in Table 1 (the fluorinated monomer and G04 content were determined by the experiments, which were shown in the Tables S1 and S2†). An appropriate amount of St, G04 (or G03, G02), KH-570, IBOMA and the initiator (BPO) were added into the flask. Then, the mixture was stirred and slowly heated to 85 °C. After the viscosity of polymer solution was increased to approximately 11 mPa s, an appropriate amount of AA and DMC were added to the system. Then the system was maintained until the viscosity of the polymer solution was increased to approximately 11 mPa s. Finally, the temperature was cooled to room temperature and the transparent viscous liquid was obtained. Based on different contents of KH-570 (wt%: 5, 10, 15) and IBOMA (wt%: 0, 10), a series of polyfluorosilicone acrylates materials were prepared and designated as FS/S-5, FS/S5, FS/S-10 and FS/S-15, respectively. Synthetic procedures (FS/S-5, FS/S5, FS/S-10 and FS/S-15) were shown in the ESI.†

2.3. Cladding technology

2.3.1 Preparation of polyfluorosilicone acrylates cladding agent. The polyfluorosilicone acrylates cladding agents (3 wt%) were prepared by diluting the polyfluorosilicone acrylates polymer solutions in DMC-EtOH solvent mixture, and the final weight ratio of the DMC-EtOH solvent mixture was 2.5 : 1.

2.3.2 Brick treatment. The old brick samples, before treatment, were washed with deionized water in order to remove dust deposits, and then dried at 60 °C for 24 h. The brick consolidant-protective treatment was performed by brush in 22 cm × 10 cm × 4 cm samples and 5 cm × 5 cm × 1 cm samples and by soak absorption for 10 min in 1 cm × 1 cm × 2 cm samples. After treatment, the brick samples were left at room temperature to release all the solvent for 3–5 days before any further tests were carried out. The exact amount of cladding agents applied on brick sample was determined by weight difference ($\approx 1.744 \text{ mg cm}^{-2}$).



2.4. Characterization

2.4.1 FTIR. The FTIR spectra of the copolymers were obtained with an AVATAR 370 FTIR spectrometer (Nicolet, USA), at a resolution of 4.000 cm^{-1} and an accumulation of 16 scans.

2.4.2 NMR analysis. The ^{19}F NMR spectra of the copolymers were obtained by a Bruker AVANCE III HD 600 MHz NMR Spectrometer (Bruker, Switzerland) using CDCl_3 as the solvent.

2.4.3 X-ray photoelectron spectroscopy (XPS). X-ray photoelectron spectra (XPS) measurements of the copolymer were performed on an ESCALAB 250Xi (Thermo Fisher Scientific, America) with $\text{Al K}\alpha$ (X-ray) lamp-house. The compositions of film-air surface were determined.

2.4.4 Gel permeation chromatography (GPC). The molecular weight and polydispersity were determined by Waters 1515 gel permeation chromatography (Waters, USA). Tetrahydrofuran (THF) was used as eluent at a flow rate of 1 mL min^{-1} . The samples were prepared dissolving 2 mg polymer in 1.2 mL THF .

2.4.5 The glass transition temperature. The glass transition temperature of the copolymers was obtained using a TA Q500 HiRes (TA Instruments, USA) differential scanning calorimeter. The scanning rate was $10\text{ }^\circ\text{C min}^{-1}$ from $-50\text{ }^\circ\text{C}$ to $250\text{ }^\circ\text{C}$ under nitrogen atmosphere.

2.4.6 The properties of the polyfluorosilicone acrylates. The viscosity of the four polymer solutions (3 wt%) was determined with an NDJ-8S numerical viscometer (Shanghai Lichen Instrument Technology Co., Ltd., China) according to ISO 2884-1974. The pencil hardness of the polymer films was measured with a QHQ-A pencil sclerometer (Zhenwei Testing Machinery Co., Ltd., China) according to ISO 15184:1998. The adhesion was measured with a QFH paint film adhesion tester according to ISO 2409:2013 by cross cut test. Impact resistance was measured with a QCJ-120 impact tester according to the standard ISO 6272-2:2011. The water contact angle of the polymer films was measured according to GB/T 30693-2014 on an OCA 15EC video-based measuring system (EASTERN-DATAPHY (HK), China). Water absorption of polymer films was measured by gravimetric variation before and after immersing the polymer films into deionized water for 24 h. The corrosion resistance to acid and alkali was carried out with water solution of 5.0 wt% sulfuric acid and 5.0 wt% sodium hydroxide respectively at room temperature for 30 d.

2.4.7 Thermogravimetric analysis (TGA). Thermogravimetric analysis was investigated at a heating rate $10\text{ }^\circ\text{C min}^{-1}$ under nitrogen atmosphere in the temperature range $25\text{--}600\text{ }^\circ\text{C}$ by TA Q500 HiRes (TA Instruments, USA).

2.4.8 UV-vis transmittance. Optical transmittance spectra of polymer films from 280-800 nm were recorded on a UV-2501PC UV-vis spectrometer (Shimadzu, Japan).

2.4.9 Assessment of antibacterial and fungistatic properties. According to *the Pharmacopoeia of the people's Republic of China*, the antibacterial and fungistatic properties of polyfluorosilicone acrylates were evaluated utilizing the method of plate-counting. The bacteria and fungi were inoculated on LB liquid medium and incubated at $37\text{ }^\circ\text{C}$ for 24 h. For these experiments, initial concentration of bacteria and fungi was set approximately 10^6 to 10^7 CFU per mL. 100 μL of initial bacteria

and fungi were added on the coated and uncoated plate and ensured the uniform distribution on the surface. After being maintained for a moment, the plates were inverted and incubated for 24 h at $37\text{ }^\circ\text{C}$. Uncoated plates containing bacterial fluid were used as the control groups.

2.4.10 Water contact angle. Water contact angle of the treated ancient bricks surface was measured using an OCA 15EC video-based measuring system (EASTERN-DATAPHY (HK), China) at room temperature (RT, $25\text{ }^\circ\text{C}$). The droplet of distilled water (5 μL) was placed on the surface of the treated brick sample, and the water contact angle test was completed within 10 seconds. Water contact angle of the sample was the average value of five measurements on different positions at the sample surface.

2.4.11 Water absorption by total immersion. The water absorption of the treated and untreated brick samples was calculated by determination of the weight for dry sample (M_1) and the weight of totally water-saturated sample for 24 h (M_2):

$$\text{Water absorption (wt\%)} = (M_2 - M_1)/M_1 \times 100\% \quad (1)$$

2.4.12 Freeze-thaw cycles test. The treated and untreated brick samples were soaked in water for 12 h, followed by freezing at $-20\text{ }^\circ\text{C}$ for 12 h after absorbing excess surface water with a filter paper. This process was repeated 50 times in this experiment.

2.4.13 Soluble salts aging test. The treated and untreated brick samples were immersed in a 10 wt% sodium sulfate (Na_2SO_4) solution for 4 h, then all the samples were taken out and allowed to stand at ambient temperature for making the salt precipitates few hours. Then all were washed with deionized water and moved to the oven under $60\text{ }^\circ\text{C}$ for 4 h. This process was repeated for 30 times in this experiment.

2.4.14 Penetration depth. The penetration depth of each cladding agents was measured by cutting the specimens vertically and moistening the cross section. The hydrophobic zone then showed up much lighter than the wet material.

2.4.15 Water vapor permeability. For the water vapor permeability, the treated and untreated brick samples were fixed on the top of containers that were partially (1/2) filled with water. Then, the containers fixed and sealed with brick were placed in a climatic chamber, kept at R.H. $40\% \pm 1$ and at constant temperature of $25 \pm 1\text{ }^\circ\text{C}$. The containers were weighted every 24 h to determine the mass of water vapor passing through the surface unit under controlled conditions. Then water vapor transmission rate (WVTR) expressed in $\text{g}(\text{m}^2\text{ d})^{-1}$ was defined as:

$$\text{WVTR} = \Delta m/(A \times t) \quad (2)$$

where: Δm is the weight change (g), A is the area exposed to water vapor (m^2), t is the time when Δm occurred (24 h). In our case, Δm was calculated as the average of five consequent values of the daily difference in weight.

2.4.16 Colorimetric measurements. The total colour difference between the treated and untreated brick samples



(ΔE^*) was evaluated by the use of $L^*a^*b^*$ coordinates of CIE 1976 scale¹⁰ and is defined as:

$$\Delta E = [(\Delta L^*)^2 + (\Delta a^*)^2 + (\Delta b^*)^2]^{1/2} \quad (3)$$

where ΔL^* is the lightness difference; Δa^* is the red/green difference; and Δb^* is the yellow/blue difference.

2.4.17 SEM analysis. Morphology of the treated and untreated brick samples was observed using an Apollo 300 scanning electron microscope (Shanghai China Science Xinxin International Trade Co., Ltd., England) at an accelerating voltage of 15 kV. All specimens were sputter-coated with gold prior to examination.

3. Results and discussion

3.1. SEM analysis

The surface morphology of the untreated brick and the brick treated with FS/S-10 was evaluated by SEM. As shown in Fig. 2a, the microstructure of the untreated brick sample was porous and incompact. After being treated with FS/S-10 cladding agent, the microstructure of brick was not obviously changed, but it did appear smoother and denser due to the formation of the cladding between the loosened grains, which improved the brick mechanical strength and weather resistance, however, part of macropores were open, which gave a specific characteristic of permitting water vapor movement through the brick.

3.2. Molecular structure of the claddings and the interaction between claddings and brick

The tested old brick samples from a historic house of Hongcun were mainly composed of quartz (SiO_2). The polymer was prepared by solution copolymerization of fluorinated acrylate monomer, silicone-containing monomer and normal acrylate monomer. The fluorine atom at the outermost surface of the cladding can effectively block liquid water and pollutants from the environment. The functional groups ($-\text{Si}-\text{OH}$ and $-\text{COOH}$) of the molecule can undergo a condensation reaction with the $-\text{OH}$ on the surface of the old brick to form a strong $\text{Si}-\text{O}-\text{Si}$ bond. In addition, the fluorine atom in the molecule and the oxygen atom of the $\text{C}=\text{O}$ in the molecule can form hydrogen bonds with the $-\text{OH}$ on the surface of the old brick. These chemical bonds and intermolecular forces can make the cladding firmly covered on the microstructure of shallow surface

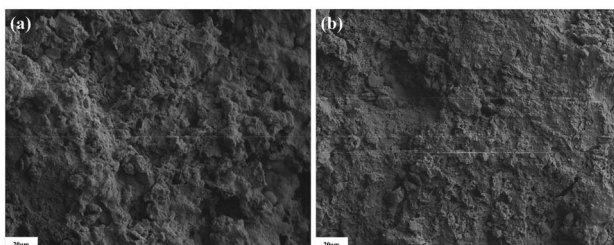


Fig. 2 SEM images of (a) the untreated brick sample and (b) the brick sample treated with FS/S-10.

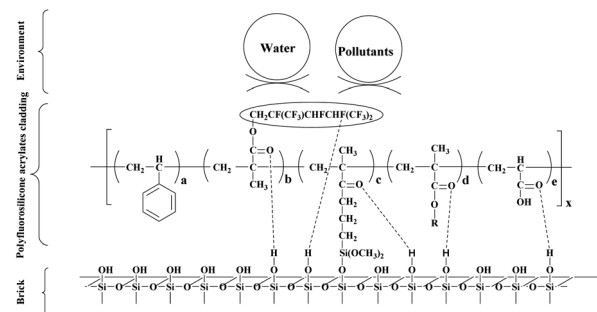


Fig. 3 Schematic diagram of the interaction between the cladding and the brick.

layer of old brick. Schematic diagram of the microstructure of the interaction between the cladding and the brick was shown in Fig. 3.

3.3. Characterization of the polyfluorosilicone acrylates

Fig. 4 showed FT-IR spectra of the four polyfluorosilicone acrylates. Herein, FS/S-10 was discussed as an example. It showed the characteristic stretching vibration of $\text{C}-\text{H}$ (CH_3) at 2947 cm^{-1} , stretching vibration of $\text{C}=\text{O}$ at 1726 cm^{-1} , stretching vibration of $\text{C}-\text{F}$ at 1246 and 1173 cm^{-1} , stretching vibration of $\text{Si}-\text{O}-\text{Si}$ at 1102 cm^{-1} , stretching vibration of $\text{C}=\text{C}$ (aromatic ring) at 1600 cm^{-1} , bending vibration of $\text{C}-\text{H}$ (aromatic ring) at 701 and 759 cm^{-1} , and bending vibration of CH_3 at 1455 and 1380 cm^{-1} . Besides, peaks at 1680 – 1620 cm^{-1} related to $\text{C}=\text{C}$ were disappeared completely, confirming that all of the monomers were copolymerized into the copolymers. The exact FTIR spectra analyses of the other polyfluorosilicone acrylates were available in the ESI.†

Fig. 5 showed ^{19}F NMR spectra of the fluorinated monomers and the four polyfluorosilicone acrylates. The peaks at -72 to -76 ppm , -185 to -190 ppm and -208 to -212 ppm were attributed to $-\text{CF}_3$ group, $-\text{CHF}-$ group, and $-\text{CH}_2\text{CF}-$ group, respectively. It was clear that all the copolymers showed almost

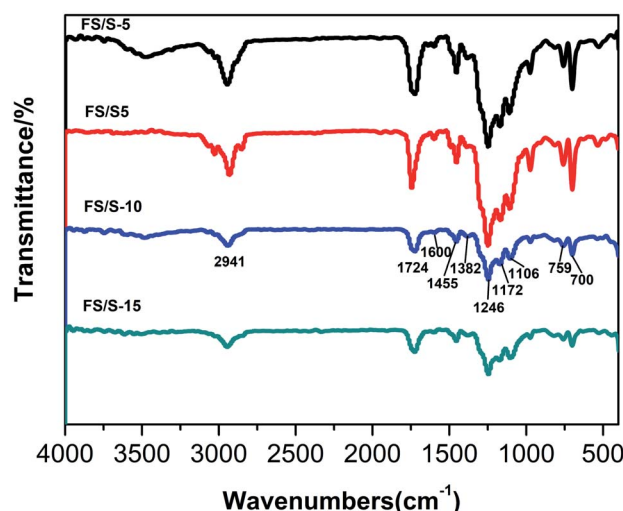


Fig. 4 FTIR spectra of FS/S-5, FS/S5, FS/S-10 and FS/S-15.



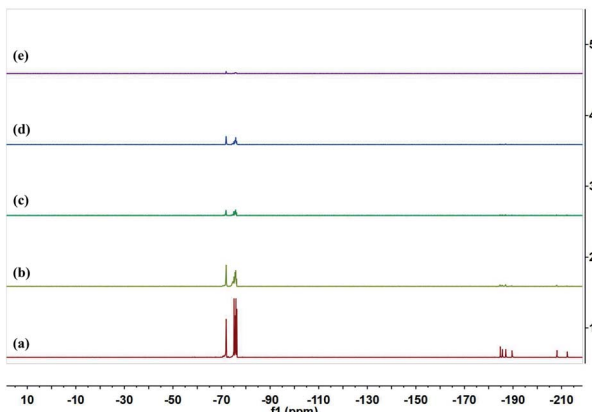


Fig. 5 ^{19}F NMR spectra of (a) G04, (b) FS/S-5, (c) FS/S5, (d) FS/S-10, and (e) FS/S-15.

the same peaks as those of G04. The results indicated that the fluorinated monomer had participated in the polymerization. However, the fluorine peaks of the polyfluorosilicone acrylates were weaker than those of G04 and dramatically decreased with the increment of KH-570 content. This might be due to the relatively less amount of fluorine component dissolved in CDCl_3 . The exact ^{19}F NMR spectra analyses of the four polyfluorosilicone acrylates were available in the ESI.†

XPS is used to analyze the surface chemical compositions of polymer. The full-scan XPS spectra and the surface elements analysis diagram of FS/S-5 were revealed in Fig. 6 and Fig. 7.

The peak at 688 eV assigned to F (1s), the peak at 532 eV assigned to O (1s), the peak at 285 eV assigned to C (1s), the peak at 168 eV assigned to Si (2s) and the peak at 102 eV assigned to Si (2p) were observed in the spectrum of FS/S-5, indicating that both the fluorinated monomer and the silicone-containing monomer were chemically bonded into the FS/S-5. The number percentage of F, O, C, Si in the film-air interface of FS/S-5 were 23.69%, 9.08%, 66.29% and 0.94%. However, the theoretical percentages of F and Si in the bulk were 12.59% and 0.28%. This suggested that the fluorinated

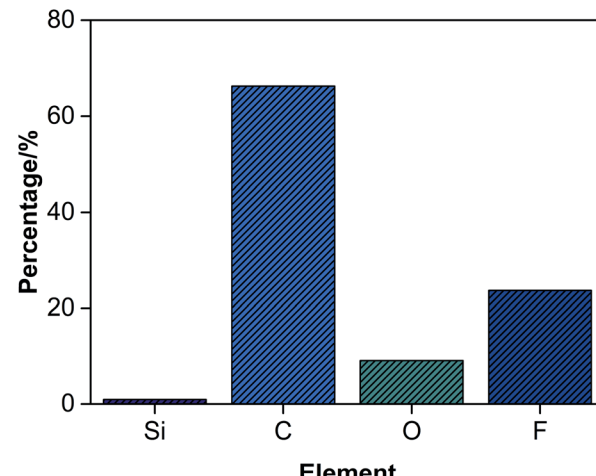


Fig. 7 The element content of FS/S-5.

Table 2 The molecular weight of the polyfluorosilicone acrylates

Sample	$M_n/10^4$	PDI
FS/S-5	5.8	2.0
FS/S5	6.1	1.7
FS/S-10	6.6	1.6
FS/S-15	6.8	1.8

and silicon-containing segments had migrated to the film-air interface.

M_n values of all the copolymers were close to each other in the range of 58 000 and 68 000 (Table 2), suggesting that these copolymers show their solubility, adhesion, weather resistance, hardness, and penetrability in a uniform consistent mode.¹¹

DSC was employed to test the T_g of the copolymers to judge the homogeneity of the copolymerization process.¹² It was apparent that each copolymer exhibited only one T_g , indicating that all of the monomers had been successfully copolymerized into the expected FS/S-5, FS/S5, FS/S-10 and FS/S-15.

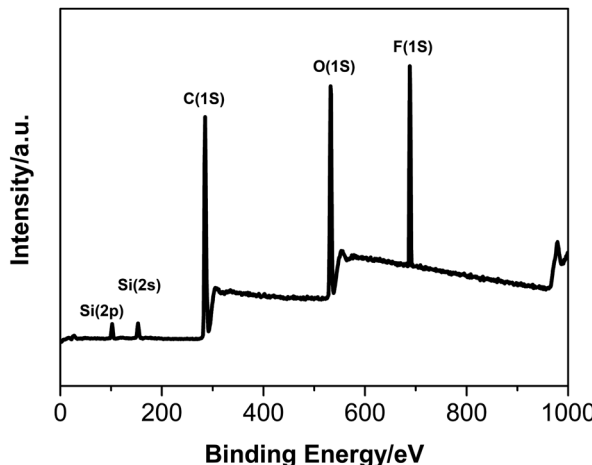


Fig. 6 XPS spectra of FS/S-5.

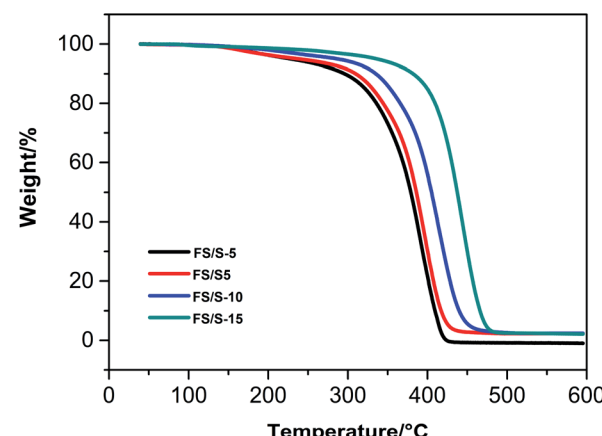


Fig. 8 TGA curves of different polyfluorosilicone acrylates copolymers.



Table 3 Properties of the polyfluorosilicone acrylates copolymers

Properties	Sample			
	FS/S-5	FS/S5	FS/S-10	FS/S-15
Viscosity (mPa s)	15	18	20	22
Pencil hardness (100 °C) ^a	6H	6H	6H	6H
Adhesion ^b	Gt 0	Gt 0	Gt 0	Gt 0
Impact resistance (cm) ^b	50	50	50	50
Contact angle (°) ^c	99	100	99	95
Water absorption (wt%) ^c	5.92	5.56	1.12	1.14
5 wt% NaOH (30 d) ^c	Unchanged	Unchanged	Unchanged	Unchanged
5 wt% H ₂ SO ₄ (30 d) ^c	Unchanged	Unchanged	Unchanged	Unchanged

^a The test was carried out with Zhong Hua advanced drawing pencils. ^b Polymer films were cast on the tinplate substrates. ^c Polymer films were cast on a glass substrate.

Furthermore, it also revealed that the T_g tended to decrease with the increment of KH-570 content, namely, 65, 66, 63 and 60 °C for the FS/S-5, FS/S5, FS/S-10 and FS/S-15, respectively (Fig. S3†). This may be due to the increment of the flexible Si–O–Si bond with the increasing KH-570 content.

In conclusion, all the fluorinated monomers, silicone-containing monomers and normal acrylate monomers had participated in the reaction.

3.4. The properties of the polyfluorosilicone acrylates copolymers

As shown in Table 3, the results of viscosity, hardness, adhesive property, mechanical property, hydrophobic property and corrosion resistance of the four copolymers were all pretty good and were better than those of core–shell fluoroacrylate copolymer latexes reported by He *et al.*¹³

3.5. The thermal properties of the polyfluorosilicone acrylates copolymers

TGA analysis results of the polymer films were shown in Fig. 8. Results showed that when increasing the KH-570 content from 5 wt% to 15 wt%, the initial degradation temperature ($T_{d, 5\%}$) increased from 228 to 336 °C, indicating that the thermal

stability of the copolymers was significantly improved with the increment of KH-570 content. This was because the high bond energy of Si–O–Si and the enhanced cross-linked silica network arising from the hydrolysis and condensation of Si(OR)₃ groups. By contrast with the UV-cured fluorinated siloxane graft copolymer studied by Yan *et al.*,¹⁴ the polyfluorosilicone acrylates prepared in this work had better thermal stability.

3.6. UV-vis transmittance property of the polyfluorosilicone acrylates copolymers

UV-vis transmittance analysis results of the polymer films were reported in Fig. 9. The transmittance during ultraviolet region from 200 to 400 nm in all the polymer films was approximately 0%, which can protect the brick from photo-degradation due to the UV-radiation. Furthermore, the four copolymer films all showed high transmittance of approximately 100% in the visible region (400–800 nm), which endowed the copolymers good optical properties to preserve the initial brick colour.

3.7. The antibacterial and fungistatic properties of the polyfluorosilicone acrylates copolymers

According to the *Pharmacopoeia of the people's Republic of China*, the antibacterial and fungistatic properties of polyfluorosilicone acrylates against *Staphylococcus aureus* (*S. aureus*), *Escherichia coli* (*E. coli*) and *Candida albicans* (*C. albicans*) were evaluated utilizing the method of plate-counting. Each experiment was carried out in duplicate and the mean results were demonstrated in Table 4.

The results demonstrated that the four polyfluorosilicone copolymers had satisfactory antibacterial and fungistatic properties.

3.8. Preliminary evaluation of consolidant and protective treatment on old brick

Protective materials for brick wall of a historic house need to have hydrophobic properties to prevent water penetration into the bulk of the brick.¹⁵ Thus, the hydrophobic properties of the treated brick samples based on their water contact angle and water absorption were investigated.¹⁶ Water droplets were dripped on the untreated brick surface and the treated brick

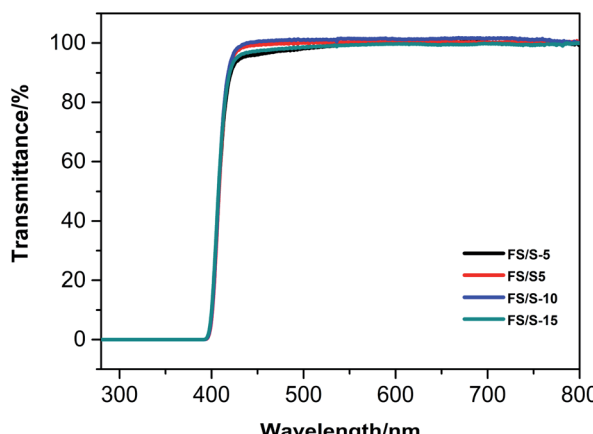


Fig. 9 UV-vis spectra of different polyfluorosilicone acrylates copolymers.



Table 4 Antibacterial and fungistatic properties of Nippon Paint Odour-less 120 (2-in-1) Interior Emulsion Paint and polyfluorosilicone acrylates polymer against *S. aureus*, *E. coli* and *C. albicans*^a

Sample	Total number of colonies per square centimeter		
	<i>E. coli</i>	<i>C. albicans</i>	<i>S. aureus</i>
Bacterial fluid	1645	1645	1645
Nippon Paint Odour-less 120 (2-in-1) Interior Emulsion Paint	16.4	16.5	164.5
FS/S-5	—	—	0.016
FS/S5	—	—	0.018
FS/S-10	—	—	0.013
FS/S-15	—	—	0.020

^a “—” no colony was observed.

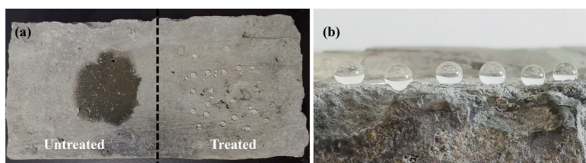


Fig. 10 (a) Comparison diagram of water droplets deposited on the surface of the brick sample before and after consolidant-protective treatment; (b) the close-up of water droplets deposited on the surface of the treated brick sample.

surface. As shown in Fig. 10a, the water droplets spread on the untreated surface of the brick and were immediately absorbed by the substrate, while water droplets deposited on the treated surface of the brick could maintain nearly spherical shape. The water contact angle of the FS/S-5, FS/S5, FS/S-10 and FS/S-15 treated surface of old brick reached to 135, 134, 133 and 130°, respectively. It is obviously found that the water contact angles of treated brick sample decreased slightly with increment of KH-570 content. It was because that the high degree of cross-linking network will hinder more hydrophobic fluorinated segment orientating to film-air interface when the KH-570 content exceeded up to 5 wt%.¹⁷ As shown in Fig. 11b, the

water absorption of untreated bricks was 16.1 wt%, while the water absorption of the treated brick sample was sharply descended down to 2.8 wt% and 2.7 wt% when the KH-570 content increases to 10 wt% and 15 wt%. This could be explained that the high degree of crosslinking network resulted by the hydrolysis and condensation of Si(OR)₃ prevented the water infiltration on some level. Compared with alkoxy silane in Stefanidou's work,¹⁸ the water resistance of brick sample treated with FS/S-10 and FS/S-15 was greatly improved.

The repeated freezing and thawing of water absorbed inside the old bricks may create pressure on the porous brick, which eventually can lead to cracks in bricks.¹⁹ As shown in Table 5, resistance to freeze-thaw of the brick samples treated with different cladding agents increased to varying degrees compared with the untreated brick sample, among which, the FS/S-10 and FS/S-15 treated sample exhibited pretty good freeze-thaw resistance. No obvious change was observed for brick samples treated with FS/S-10 and FS/S-15 after 50 freeze-thaw cycles. By contrast with silicone resin in Zielecka's work,²⁰ the polyfluorosilicone acrylates in this work exhibited relatively better freeze-thaw resistance. The exact weight loss after the freeze-thaw cycles test was shown in the ESI (Fig. S4).†

Under supersaturated conditions, the growing crystals of a salt solution exert pressure against the pore-walls, known as

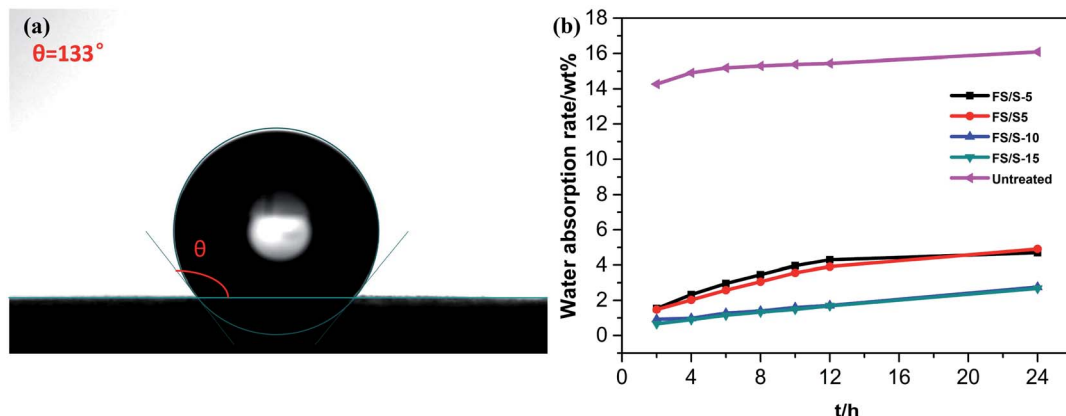


Fig. 11 (a) Water contact angle of the surface of the brick sample treated with FS/S-10; (b) the water absorption by total immersion of brick samples treated with different cladding agents.



Table 5 Properties of untreated and treated brick samples

Samples	Freeze-thaw cycles	Soluble salts aging cycles	Penetration depth (mm)	Water vapor permeability (g per m ² per 24 h)	ΔE
Untreated	8	6	—	2.87	—
FS/S-5	24	9	15	2.66	0.94
FS/S5	34	12	14.5	2.68	0.83
FS/S-10	50	30	14.5	2.72	1.01
FS/S-15	50	30	14	2.74	1.22

crystallization pressure, causing damage to the brick.²¹ As shown in Table 5, under soluble salts aging test, the samples treated with FS/S-5, as well as the untreated brick, cracked in cross-section after only 9 and 6 cycles, respectively. The surfaces of old brick samples treated with FS/S5 flaked slightly after 12 cycles during soluble salts aging test. However, no obvious change was observed for FS/S-10 and FS/S-15 treated brick sample after 30 soluble salts aging cycles. Compared with the silicic acid ester,^{22,23} the polyfluorosilicone acrylates exhibited better resistance to soluble salts aging. The exact weight loss after the soluble salts aging test was shown in the ESI (Fig. S5).†

It is widely accepted that the penetration depth of cladding is an important parameter to be taken into account when assessing consolidation effectiveness.²³ Table 5 showed that the penetration depth of claddings in brick samples decreased slightly with increment of KH-570 content, which was attributed to the increased viscosity of the cladding agent. However, the penetration depth of the four cladding agents was acceptable.

The water vapor transmission rates through the brick should not be reduced after treatment, assuring the proper vapor regime inside the brick and the historic house. The impermeability of the cladding to water vapor can lead to water condensation just underneath the cladding, which may accelerate the brick's decay.²⁴ Table 5 showed that the water vapor permeability of the treated brick samples increased slightly with the increase of KH-570, which probably due to that the cross-linking network originating from the hydrolysis of the siloxane ensured the water vapor permeability of the brick.

The results of colorimetric measurements summarized in Table 5 indicated that the application of the cladding agents did not have any considerable optical effect on the aesthetic appearances of the old brick. Furthermore, the applications of the claddings led to colour changes in brick which were not perceived by the human eye ($ΔE^* < 1.5$). The exact color differences are available in the ESI (Table S4).†

4. Conclusions

Overall, polyfluorosilicone acrylates (FS/S-10) seems to be placed as the most suitable material for the consolidation and protection of the brick wall in a historic house, since the cladding made from the FS/S-10 permeated through the surface of old brick with an average depth of 14.5 mm in this case study, and provided ultrathin and efficient covering of microstructure of shallow surface layer of old bricks and resulted excellent water-proof, moisture-proof, mildew-proof and long-lasting

weather resistance effects with good hydrophobicity, mechanical strength, thermal resistance, chemical resistance, antibacterial and fungistatic properties. The water contact angle of treated surface of old bricks reached to 133°, the water absorption of treated bricks was descended down from 16.1 wt% to 2.8 wt% after soaking in water for 24 h. The good results obtained with the fluorosilicone polyacrylate cladding as a consolidant and protective material of brick wall of historic house, facile and cost-effective synthetic process and its simple and environmental application imply their potential for the conservation of historic brick buildings.

Conflicts of interest

There are no conflicts to declare.

Acknowledgements

The Government of Yixian County of Anhui Province is highly appreciated for support of this research project.

References

- 1 H. Zhang, Q. Liu, T. Liu and B. Zhang, *Prog. Org. Coat.*, 2013, **76**, 1127–1134.
- 2 P. Maravelaki-Kalaitzaki, N. Kallithrakas-Kontos, D. Korakaki, Z. Agioutantis and S. Mauriannakis, *Prog. Org. Coat.*, 2006, **57**, 140–148.
- 3 C. D. Vacchiano, L. Incarnato, P. Scarfato and D. Acierno, *Constr. Build. Mater.*, 2008, **22**, 855–865.
- 4 A. P. Ferreira Pinto and J. Delgado Rodrigues, *J. Cult. Herit.*, 2012, **13**, 154–166.
- 5 P. Maravelaki-Kalaitzaki, N. Kallithrakas-Kontos, Z. Agioutantis, S. Mauriannakis and D. Korakaki, *Prog. Org. Coat.*, 2008, **62**, 49–60.
- 6 M. Mosquera, J. Pozo and L. Esquivias, *J. Sol-Gel Sci. Technol.*, 2003, **26**, 1227–1231.
- 7 F. Xu, W. Zeng and D. Li, *Prog. Org. Coat.*, 2019, **127**, 45–54.
- 8 P. Li, F. Qiu, X. Zhang, L. Wang, Q. Chen and D. Yang, *J. Polym. Eng.*, 2015, **35**, 511–522.
- 9 X. Zhang, W. Wen, H. Yu, Q. Chen, J. Xu, D. Yang and F. Qiu, *Chem. Pap.*, 2016, **70**, 1621–1631.
- 10 G. Cappelletti, P. Fermo, F. Pino, E. Pargoletti, E. Pecchioni, F. Fratini, S. A. Ruffolo and M. F. La Russa, *Environ. Sci. Pollut. Res.*, 2015, **22**, 17733–17743.



11 B. Su, H. Zhang, B. Zhang, D. Jiang, R. Zhang and X. Tan, *J. Cult. Herit.*, 2018, **31**, 105–111.

12 K. Landfester, R. Rothe and M. Antonietti, *Macromolecules*, 2002, **35**, 1658–1662.

13 L. He and J. Liang, *J. Fluorine Chem.*, 2008, **129**, 590–597.

14 Z. Yan, W. Liu, N. Gao, H. Wang and K. Su, *Appl. Surf. Sci.*, 2013, **284**, 683–691.

15 Y. Liu and J. Liu, *Constr. Build. Mater.*, 2016, **122**, 90–94.

16 C. Kapridaki and P. Maravelaki-Kalaitzaki, *Prog. Org. Coat.*, 2013, **76**, 400–410; M. Lettieri, M. Masieri, A. Morelli, M. Pipoli and M. Frigione, *Coatings*, 2018, **8**, 429.

17 X. Cui, S. Zhong and H. Wang, *Polymer*, 2007, **48**, 7241–7248.

18 M. Stefanidou and A. Karozou, *Constr. Build. Mater.*, 2016, **111**, 482–487.

19 D. Kronlund, M. Lindén and J.-H. Smått, *Constr. Build. Mater.*, 2016, **124**, 1051–1058.

20 M. Zielecka and E. Bujnowska, *Prog. Org. Coat.*, 2006, **55**, 160–167.

21 X. Zhang, W. Wen, H. Yu, F. Qiu, Q. Chen and D. Yang, *J. Polym. Res.*, 2016, **23**, 75.

22 I. Karatasios, P. Theoulakis, A. Kalagri, A. Sapalidis and V. Kilikoglou, *Constr. Build. Mater.*, 2009, **23**, 2803–2812.

23 Y. Luo, L. Xiao and X. Zhang, *J. Cult. Herit.*, 2015, **16**, 470–478.

24 P. N. Manoudis, A. Tsakalof, I. Karapanagiotis, I. Zuburtikudis and C. Panayiotou, *Surf. Coat. Technol.*, 2009, **203**, 1322–1328.

